AGU PUBLICATIONS

Water Resources Research

RESEARCH ARTICLE
10.1002/2016WR019146

A new classification scheme of European cyclone tracks with relevance to precipitation

M. Hofstätter[1], B. Chimani[1], A. Lexer[1], and G. Blöschl[2]

[1]Climate Research Department, Central Institute for Meteorology and Geodynamics, Vienna, Austria, [2]Institute of Hydraulic Engineering and Water Resources Management, Vienna University of Technology, Vienna, Austria

Key Points:
- Cyclones identified from atmospheric pressure maps account for 47%–76% of precipitation in central Europe
- The risk of heavy precipitation strongly depends on the cyclone track type, with the Vb type producing the highest precipitation rates
- Vb summer cyclones are particularly strong and account for most of the major precipitation events in the Czech Republic during 1961–2002

Correspondence to:
M. Hofstätter,
m.hofstaetter@zamg.ac.at

Citation:
Hofstätter, M., B. Chimani, A. Lexer, and G. Blöschl (2016), A new classification scheme of European cyclone tracks with relevance to precipitation, *Water Resour. Res.*, *52*, 7086–7104, doi:10.1002/2016WR019146.

Received 3 MAY 2016
Accepted 20 AUG 2016
Accepted article online 25 AUG 2016
Published online 21 SEP 2016

Abstract This paper proposes a new classification scheme of atmospheric cyclone tracks over Europe. The cyclones are classified into nine types, based on the geographic regions, the cyclones traverse before entering central Europe. The method is applied to ERA-40 data for 1961–2002, considering all significant cyclones above a relative vorticity threshold. About 120 and 80 cyclone tracks per year are identified at sea level pressure and 700 hPa geopotential height, respectively. About 25% are Atlantic type cyclones, 25% emerge directly over central Europe, and another 25% originate from the lee of the Alps. The other types are less frequent (Mediterranean 12%, Polar 7%, Continental 2%, and Vb 4%). The track types show distinct characteristics in terms of cyclone intensity and cyclone life stage when entering central Europe. Cyclones of type Vb are, on average, the most intense cyclones over central Europe and even more intense than Atlantic cyclones in summer, pointing to their potential for generating extreme precipitation. The identified cyclones account for 46%–76% of long-term precipitation in a focus region in central Europe. Precipitation differs significantly between cyclones, with Atlantic and Vb cyclones producing the highest and Continental and Polar cyclones producing the lowest long-term precipitation totals. The contributions of cyclone types to total precipitation show distinct spatial patterns within central Europe. The new cyclone type catalog will be useful for identifying the relevance of specific track types for precipitation extremes in central Europe and analyze their temporal behavior in the context of climate change.

1. Introduction

Midlatitude cyclones play an essential role in maintaining the global atmospheric energy balance by the exchange, transport, and transformation of mass, energy, and momentum. The cyclones are associated with a range of local weather phenomena including extreme windstorms and precipitation. As early as 1891, van Bebber recognized the role of a specific cyclone track type in generating heavy, large-scale precipitation and winter snowstorms in central Europe [*van Bebber*, 1891]. He attributed several of these events to cyclones that propagate from northern Italy to Poland, leaving the Alps on the left (type Vb, read "five b"). His analysis was based on manually tracking barometric minima over time from surface weather maps for the years 1876–1890, resulting in one of the first subjective classifications of cyclone tracks in the Atlantic-European region. Some of the most devastating European floods have indeed been associated with Vb or similar type cyclones such as the August 2002 flood [*Ulbrich et al*., 2003] and the June 2013 flood [*Kummli*, 2014; *Schröter et al*., 2014; *Blöschl et al*., 2013], as well as with Vc-type cyclones in eastern Europe [*Apostol*, 2008]. The Vc type is less well known and represents all cyclones propagating from south of the Alpine ridge straight to the east. *Renard and Lall* [2014] related floods in Mediterranean France to geopotential heights and found the temporal flood variability to be associated with a particular spatial pattern in the geopotential heights. On the other hand, gale-force winds in western-Continental Europe are usually caused by cyclones that propagate from the north-eastern Atlantic into Europe [*Hanley and Caballero*, 2012; *Donat et al*., 2010], such as storm Kyrill in January 2007 and storm Lothar and Martin in December 1999 [*Roberts et al*., 2014]. Clearly, the geographical region from where a cyclone enters Europe plays an important role in generating specific weather extremes.

One of the earliest classification studies (apart from van Bebber's) focusing on dominant paths of cyclones in the Northern Hemisphere was carried out by *Klein* [1957]. In a more recent study, *Davis et al*. [1993] classified cyclones over the north-western Atlantic Ocean into distinct types, based on the depression's origin,

track, and intensification during the storm's lifetime. They defined eight types and analyzed them with regard to their potential for coastal damages. This was probably the first study that directly related the occurrence of hazardous weather events to specific classes of cyclones by considering the source regions and tracks as input information for separating types.

A more objective analysis of track types in the Atlantic-European region was performed by *Blender et al.* [1997], using a clustering approach to classify North Atlantic cyclones into three groups depending on the average direction of movement of the storm ("stationary," "zonally," and "north-eastward"). Mediterranean storm tracks may also be important as pointed out by *Bengtsson et al.* [2006] and *Hoskins and Hodges* [2002], who identified a dominant cluster of intense winter cyclones ranging from the western to the eastern Mediterranean. A similar track type emerging from the North Mediterranean and propagating to the east was identified by *Dacre and Gray* [2009] and *Trigo et al.* [1999]. *Horvath et al.* [2008] classified North Mediterranean cyclone tracks into four types ("Genoa," "Adriatic," "twin," and "others") depending on the region of origin, and *Wernli and Schwierz* [2006] found most central European winter cyclones to emerge either in the north-eastern or the northern Atlantic region.

Thus, cyclones appear to occur along preferred atmospheric "streams," with distinct thermodynamic and dynamic characteristics. For example, cyclones emerging from the Genoa region are mainly deep depressions at the most intense stage [*Campins et al.*, 2006] with a large fraction of cold-core type cyclones [*Campins et al.*, 2011].

Notwithstanding the large number of tracking studies in the literature, we are unaware of any study that focused on different types of cyclones propagating to central Europe. Such a stratified analysis would be very useful for better understanding the role of cyclone tracks in generating high impact weather extremes such as precipitation. The aim of this paper therefore is to present a new approach to classifying atmospheric cyclones over Europe and relate the identified cyclones to long-term precipitation totals. The precipitation analysis focuses on central Europe. Cyclone tracks are determined by the tracking procedure of *Murray and Simmonds* [1991] and *Simmonds et al.* [1999] with some refinements for the purpose of this study. Inspired by the early work of *van Bebber* [1891], the identification of track types is based on the geographic regions the cyclones traverse before entering central Europe. The identification by region is motivated by the expectation of preferred pathways of cyclones over Europe, so-called atmospheric streams. The resulting track types are analyzed in terms of within-type cyclone characteristics, including precipitation.

2. Developing a Classification of European Cyclone Tracks

2.1. Data

In this study, ERA-40 data [*Uppala et al.*, 2005] are used, covering the time period January 1961 to August 2002. The temporal resolution is 6 h with a spatial resolution of 1.125° (Table 1).

As atmospheric cyclones do not necessarily extend through the entire depth of the atmosphere and the vertical axis of troughs can be tilted, cyclone tracks at different atmospheric levels may be different despite being related to the same main trough. Tracks of Vb-type cyclones have traditionally been identified from sea level pressure (SLP) using hand-drawn synoptic maps. However, surface pressure patterns are strongly influenced by surface topography or boundary layer processes and may therefore contain short lived and highly variable low-pressure systems, which are not relevant for significant weather events. At higher

Table 1. Overview of Data Used in This Study

Data Set	Parameters	Spatial Coverage	Resolution	Temporal Extent	Source
ERA-40	Geopotential height and relative vorticity at 700 and 500 hPa	Global	Six-hourly, T159 (∼125 km)	1 Sep 1957 to 31 Aug 2002	European Centre for Medium Range Weather Forecasting [*Uppala et al.*, 2005]
WETRAX precipitation	Daily precipitation totals	Germany, Austria (Switzerland and Czech Republic in parts, see Figure 10)	Daily, 6 km × 6 km regular grid	1 Jan 1961 to 31 Dec 2006	*Hofstätter et al.* [2015]
Flood-related precipitation events	Significant precipitation: date and rank	Major central European rivers	River catchments	1 Jan 1951 to 31 Dec 2002	*Müller et al.* [2009]

atmospheric levels, the fields tend to be smoother, so tracks are more clearly defined. To better understand the differences between levels, cyclones are investigated independently at two levels in this paper: at sea level (using sea level pressure fields, SLP) and at the pressure level of 700 hPa (using the respective geopotential heights, GPH700 or Z).

The ERA-40 data are interpolated to an equidistant 80 km × 80 km grid by polynomials [*Akima*, 1978, 1996]. The final grid is centered on 5°E and 50°N, ranging from about 40°W to 50°E at 65°N and 20°W to 40°E at 30°N. In order to exclude small-scale or spurious systems, the data are filtered by a discrete spatial low-pass filter [*Freser and von Storch*, 2005] that removes any structures smaller than 400 km, relaxes smoothly up to 1000 km, and lets all large scales pass through [see *Hofstätter and Chimani*, 2012]. To understand the relevance of the cyclone classification for precipitation, a focus region within central Europe is selected for precipitation analysis (Germany, Austria, and parts of Switzerland and the Czech Republic). The focus region is embedded in a larger region, denoted as "Track Recognition Zone" (TRZ), to analyze precipitation with respect to the cyclone types for all cyclones moving through TRZ. Daily precipitation data on a 6 km grid are used (see Table 1) which, in case of Austria have been obtained from the Austrian Weather Service (ZAMG; the GPARD-6 data set) [*Hofstätter et al*., 2015] and for the remaining parts of the focus region from the German Weather Service (DWD; the HYRAS data set) [*Rauthe et al*., 2013].

2.2. Cyclone Tracking

The detection and tracking of cyclones in this paper is based on the concept of *Murray and Simmonds* [1991] and *Simmonds et al*. [1999] and modifications suggested by *Pinto et al*. [2005]. The tracking procedure consists of four basic elements: (a) identification of significant cyclones at time t_n, (b) prediction of a subsequent cyclone position at time t_{n+1}, (c) association of cyclones between times t_n and t_{n+1} by scoring the difference between the predicted (first guess, "FG") and all present cyclone positions (candidate points, "CP") from the data at time t_{n+1}, and (d) removal of spurious tracks. Similar to the authors mentioned above, both closed and open depressions are considered. Additionally, the following refinements have been made in the tracking procedure: (i) the association procedure not only considers the distance between *FG* and *CP* but also the angle between the propagation vectors to *FG* and *CP*. (ii) Splitting and merging of cyclone tracks is permitted, which is of importance in the classification where the tracks are investigated with regard to their source region.

First, cyclones are identified by detecting local minima of geopotential height or air pressure. We identify closed cyclones where pressure or geopotential height is lower than at the four surrounding grid points and open cyclones where it is lower at three grid points and equal or higher at the fourth point. As a measure of intensity, geostrophic relative vorticity ξ is used for SLP and GPH700

$$\xi_{\mathrm{SLP}} = \left(\frac{1}{\rho f} * \nabla^2 p\right) \text{ or } \xi_{\mathrm{GPH}} = \left(\frac{1}{f} * \nabla^2 Z\right) \tag{1}$$

where f is the Coriolis parameter and ρ is the air density. All cyclones below a minimum intensity ξ_{min} are disregarded. This threshold is set to 3.8×10^{-5} s^{-1} for open and 2.9×10^{-5} s^{-1} for closed systems in the case of SLP and 3.5×10^{-5} s^{-1} and 2.6×10^{-5} s^{-1} in the case of GPH700. The intensity thresholds are slightly higher than those of *Pinto et al*. [2005] and *Lim and Simmonds* [2007], which is consistent with the calculation of $\nabla^2 p$ and $\nabla^2 Z$ within a comparatively small radius of 160 km. Only the most intense open system along the same trough axis is considered in this study, whereas several systems have been considered by *Pinto et al*. [2005].

Second, the subsequent position (first guess, "FG") of a cyclone at time t_{n+1} is predicted through a propagation vector $\mathbf{U}_{\mathrm{pred}}$, calculated as two components. The first component, $\mathbf{U}_{\mathrm{pst}}$, takes into account continuity in cyclone propagation [*Murray and Simmonds*, 1991]. For existing tracks, $\mathbf{U}_{\mathrm{pst}}$ is therefore set to the previous displacement vector, and for new tracks, the climatological cyclone propagation at the respective grid point $\mathbf{U}_{\mathrm{pst}}$ is used. The climatological cyclone propagation is derived from an existing track catalog for the period 1961–2002 [*Hofstätter and Chimani*, 2012] and updated here by the analysis of SLP. The second component uses steering winds $\mathbf{U}_{\mathrm{low}}$ from the level of interest (700 hPa or SLP) as well as $\mathbf{U}_{\mathrm{upp}}$ from the respective upper level (500 or 700 hPa) referring to *Simmonds et al*. [1999]. $\mathbf{U}_{\mathrm{upp,\ low}}$ is estimated as the associated averaged gradient of p calculated within a radius of 320 km around the cyclone center in case of SLP and is

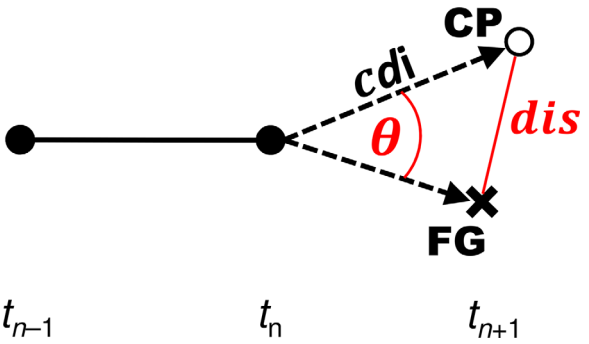

Figure 1. Schematic showing the concept of cyclone association between times t_n and t_{n+1} by assessing the distance (*dis*) between the predicted cyclone position (FG) and a candidate cyclone (CP), the angle (θ) between the propagation vectors (dashed) of CP and FG as well as the distance (*cdi*) between the cyclone position at time t_n and a CP at time t_{n+1}.

approximated by the geostrophic wind vector $\mathbf{U}_{grd}=f^{-1}(\hat{\boldsymbol{e}}_3\times\nabla Z)$ elsewhere. The two components are weighted to obtain the predicted propagation vector $\mathbf{U}_{pred}$ as given by equation (2):

$$\mathbf{U}_{pred}=(1-w_1)\cdot\mathbf{U}_{pst}+ w_1\cdot\{w_2\cdot\mathbf{U}_{low}+(1-w_2)\cdot(f_{red}\cdot\mathbf{U}_{upp})\} \quad (2)$$

The weight w_1 was set to 0.60 following *Simmonds et al.* [1999], and w_2 to 0.33 respectively, to put more emphasis on upper level winds for the latter. The reduction factor f_{red} accounts for the decrease of wind speed from upper to lower atmospheric levels [*Simmonds et al.*, 1999]. ERA-40 data over Europe suggest a typical ratio of 0.65 between $\mathbf{U}_{grd}$ at GPH500 and GPH700 (0.80 for GPH700 and SLP). For clarity, f_{red} is set to 0.7 at both levels.

Third, cyclones are connected between adjacent time steps t_n and t_{n+1}, if the association score C is larger than a threshold. This score is a measure of consistency between the candidate cyclone positions ("CP") and the predicted (first guess, "FG") position at time t_{n+1} (see Figure 1). The concept of cyclone association using scores is similar to that of *Murray and Simmonds* [1991] and *Pinto et al.* [2005], with the difference that here not only the best candidate is selected to form a track, but all candidates with scores above the threshold are selected. This entails the formation of cyclone splits and/or mergers for some tracks. As another refinement, the score C is not simply the Euclidian distance between CP and FG but consists of two parts

$$C=C_{dis}+C_{dir} \quad (3)$$

where C_{dis} is related to the distance (dis) between CP and FG and varies between 0 and 1. C_{dir} is related to the angle (θ) between the propagation vectors to FG and CP and varies between -0.15 and $+0.25$. To avoid poorly defined angle scores for slowly moving cyclones, C_{dir} is reduced to zero if the distance between CP and the cyclone location at time t_n (see Figure 1) approaches zero (equation 4c). In this work, C_{dir} is introduced to put more weight on a correct prediction of the propagation direction, to avoid cases where a similar distance would lead to the same result although the direction might be very different. The threshold of C, above which CPs are accepted to be connected to form a track, was set to 0.5 as a result of extensive testing and comparison of tracks with well-documented case studies. The scores are calculated by equation 4:

$$C_{dis}=\begin{cases}\left[1-\left(\frac{dis}{d_{max}}\right)^2\right]^{2.5} & (0\le dis\le d_{max})\\ 0 & (\text{otherwise})\end{cases} \quad (4a)$$

$$\text{with } d_{max}=450\text{km}+\left[255\text{km}\times\tanh\left(\pi\times\frac{\phi}{360}\right)\right]\ (0^\circ\le\phi\le 90^\circ) \quad (4b)$$

$$C_{dir}=\left[0.25-\left(\frac{\theta}{450}\right)\right]\times\tanh\left(\pi\times\frac{cdi}{450}\right)\ (0^\circ\le\theta\le 180^\circ) \quad (4c)$$

where the units of d_{max}, *dis*, and *cdi* are km. Other studies used a constant value of the maximum association radius d_{max} such as 420 km [*Zahn and Storch*, 2008]. In equation (4b), however, the maximum distance depends on the latitude ϕ, with values between 515 and 604 km (at 30°N and 80°N, respectively), to account for faster moving cyclones at higher latitudes [e.g., *Hewson and Titley*, 2010] as higher velocities usually imply larger prediction errors of FG. In equation (4a), a distance error of, say, 160 km for a cyclone at latitude of 50°N ($d_{max}=555$ km) gives $C_{dis}=0.8$, and a directional error of, say, $\theta=45^\circ$ and $cdi=450$ km gives $C_{dir}=0.15$. This would result in an overall association score of $C=0.95$, which is above the minimum

threshold of 0.5, so the candidate point would be connected. Although equation (4a) is adapted to the ERA-40 data, it can be readily applied to other data at different spatial resolutions by changing the intercept parameter in equation ((4a)b) from 450 to 550 km for the NCAR-NCEP1 data [*Kalnay et al*., 1996], and to 350 km for the ECMWF-ERA Interim data [*Dee et al*., 2011] as has been tested in this study (not shown).

In a last step, all tracks are screened to identify and remove very unlikely tracks. Such tracks may be the result of weak gradient situations with several ill-defined cyclone centers moving around slowly and/or erratically. A second type of spurious tracks occurs at SLP near major orographic features when a strong flow aloft generates quasi-stationary troughs. Other studies [e.g., *Sinclair*, 1994, 1997] removed all "nonmobile cyclones." However, as the region over northern Italy is one of the most important cyclogenesis regions in Europe [*Trigo et al*., 2002; *Campins et al*., 2011], in this study, such tracks are detected and excluded in a more selective way. A track is considered as spurious if all of the following criteria apply: (i) short living ($\leq$ 48 h), (ii) weak intensity (ξ smaller than 33th percentile of all cyclones at the respective level), (iii) a short total track length ($<$1000 km), (iv) low average cyclone velocity ($<$38 km h^{-1}), (v) frequent large changes of propagation direction ($>$60° on average per track), and (v) track endpoint located close to the starting point ($<$500 km). This method eliminated 17% of all tracks at SLP (11% at 700 hPa). Almost all of them are located within well-defined regions south of the Alpine ridge over the Ligurian Sea, north of the Alps over southern Germany or in the vicinity of the Carpathian Mountains in Romania (not shown).

2.3. An Illustrative Example

To illustrate the cyclone detection and tracking procedure, Figure 2 shows the tracks associated with a major central European flood event in August 2002, with the day and time in UTC (ddhh) indicated.

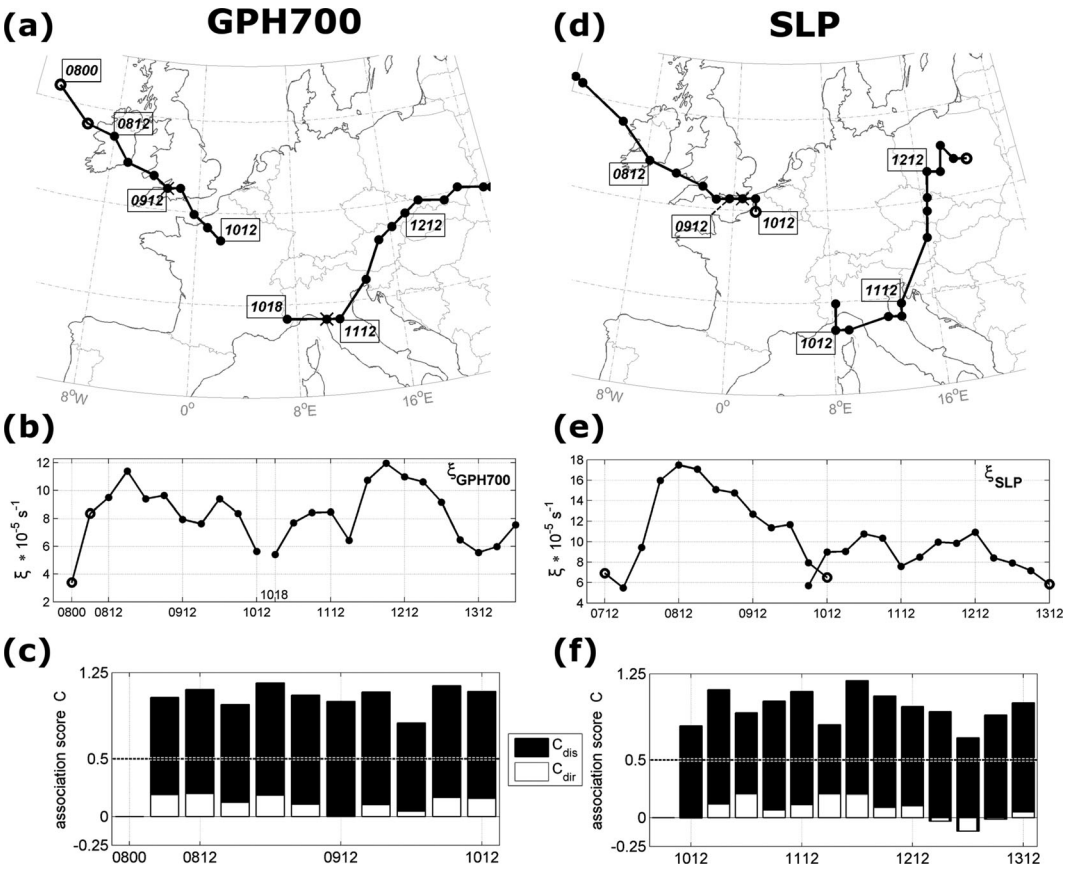

Figure 2. Cyclone track analysis for the devastating central European flood event in August 2002 at (a–c) GPH700 and (d–f) SLP. (a and d) Individual tracks with corresponding day and time in UTC (ddhh). Full and open circles indicate closed and open depressions, respectively. Positions where cyclones were found at two time steps are indicated by crosses. (b and e) Time series of relative vorticity (equation (1)). (c and f) Association score *C* (equation (3)) for the tracking of the first track at 700 hPa and the second track at SLP. The score is partitioned into directional (white) and distance (black) components. Dotted line indicates threshold C_{min} =0.5 for connecting candidate points.

The event is characterized by two individual tracks at both levels (top) interrupted at 12 UTC on 10 August. For SLP (Figure 2d), this finding is consistent with *Ulbrich et al.* [2003] who also identified two separate cyclones. At the level of 700 hPa (Figure 2a), the tracking routine also appears correct in providing two separate tracks, as the cyclone approaching from the Atlantic had weakened over the British Islands and was followed by a secondary cyclone developing in the lee of the Alps (Figure 2b). A further interesting case is point 00 UTC on 13 August at SLP (Figure 2f) where the distance is well predicted (C_{dis} = 0.78) but the direction is more than 120° off, as the cyclone changes its direction sharply. This results in a negative directional association score (C_{dir} = −0.14), reducing the total score considerably although CP and FG are close to each other. Clearly, direction adds important information to the total score, even though the total score is still above the threshold in this particular case.

2.4. Synoptically Based Classification

In this section, all cyclones reaching central Europe (CE) are classified into nine types, motivated by the expectation of preferred pathways of cyclone movement over Europe.

Separate geographical regions are defined and it is then checked whether a cyclone traverses a certain region just before moving over CE. In this study, CE is represented by a "Track Recognition Zone" (TRZ) which is set to 0.5°E–23.9°E and 42.3°N–56.2°N. Only those cyclones are considered in the following that are located in TRZ for at least 18 h. The main idea of this geographical separation is the definition of reasonably homogeneous areas with distinct climatic features, such as surface characteristics (ocean, land, and major mountain ridges) and latitude. The separation of cyclones approaching from such different regions should therefore allow the identification of track types that are systematically linked to high-impact weather events. Vb-type cyclones, for example, often develop over Genoa, very close to TRZ, and should therefore exhibit a higher relative vorticity than other track types when crossing CE.

The regions used in the classification (Figure 3) consist of the Subtropical, Atlantic, Polar, Continental, and Mediterranean regions defining five track types (STR, ATL, POL, CON, and MED), which all enter TRZ from outside. Another two track types, X-N and X-S, include cyclones emerging from one of the major source regions "nas*" or "med*" (northern Adriatic Sea or Mediterranean Sea) located inside TRZ. These rather small regions are important in terms of preferred Alpine lee-side cyclogenesis [*Buzzi and Tibaldi*, 1978; *Pichler and Steinacker*, 1987; *Trigo et al.*, 1999, 2002; *Campins et al.*, 2011]. Type X-N cyclones move to the north over the first 24 h in contrast to X-S cyclones moving to the south during the initial phase. The eighth class includes Vb cyclones which propagate from the region around northern Italy toward Poland, leaving the Alpine mountain range on the left (Figure 3b). Based on van Bebber's definition, three areas, "$x_{(t0)}$," "$x_{(tn)}$," and "in" are defined (Figure 3b), and the criteria for tracks to be classified as type Vb are chosen as follows (all criteria must apply):

1. The track is within area "$x_{(t0)}$" for at least one time step (4°E–17°E; 42°N–46°N).
2. At any later time step, the track appears in area "$x_{(tn)}$" (14°E–20°E; 47°N–55°N).

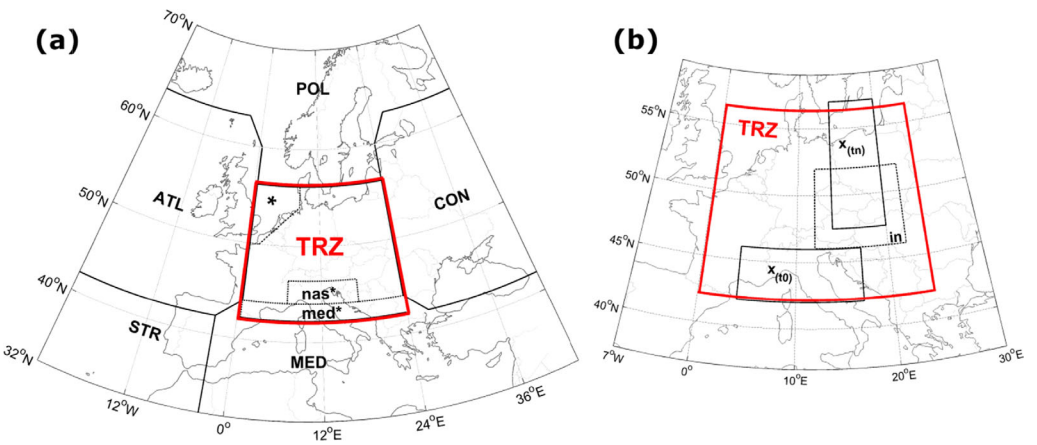

Figure 3. Regions used for the classification of cyclone tracks: (a) geographical regions determining nine different track types. TRZ (Track Recognition Zone). The small area (asterisk) in the northwest of TRZ indicates a region where newly emerging cyclones are assigned to POL or ATL, depending on the initial propagation direction. (b) Regions defining track type Vb following the original route of van Bebber (see main text for details).

Table 2. Cyclone Track Types

Priority	Acronym	Type
1	Vb	van Bebber's type "five-b"
2	X-N	Northward propagation, emerging from nas* or med*
3	X-S	Southward propagation, emerging from nas* or med*
4	MED	Mediterranean
5	STR	Subtropical
6	ATL	Atlantic
7	POL	Polar
8	CON	Continental
9	TRZ	"Track recognition zone" All tracks emerging within TRZ (except Vb, X-N, and X-S)

3. Any time between located in "$x_{(t0)}$" and "$x_{(tn)}$," the track appears in area "in" (12°E–22°E; 46°N–52°N).
4. There is an overall movement from west to east between "$x_{(t0)}$" and "$x_{(tn)}$."

The ninth class, TRZ, includes all tracks originating inside region TRZ which cannot be attributed to any other type. An exception are cyclones emerging in the small area (*) in the northwest of TRZ (Figure 3a) which are assigned to POL or ATL, if the average propagation direction in the first 18 h is between 145° and 235° or 45° and 135°, respectively.

The nine track types are assigned according to priority. Because of their relevance for flooding in central Europe, Vb is set as the highest priority. Therefore, the tracks are first tested whether they qualify for type Vb. If not, the track is subsequently tested for the other types (see Table 2). Track types X-N and X-S are set as priorities two and three, respectively, because they originate from important cyclogenesis regions close to CE.

In case of a track-complex, including cyclone mergers and/or splits, only the branch with the highest priority (Table 2) is considered. For example, if a track T_i includes a single split, the track type is assessed for each of the two subtracks T_{i1} and T_{i2} (Figure 4) independently, followed by identifying the primary track type by priority and only retaining the primary branch. Hence, all tracks considered in the following are single paths without branches. Finally, due to their very low number, STR tracks are not considered further in the statistics of this paper.

3. Track Type Characteristics

The new track type catalog offers a range of opportunities for investigating track type processes and impacts. In this section, the analysis focuses on selected climatological characteristics of the track types.

3.1. A Brief Climatology of Tracks Types

The climatological track frequency and mean propagation direction for each track type at 700 hPa are shown in Figures 5 and 6. Track frequency (shown as colors) is calculated as the number of cyclones that have been recognized at each grid point during the period 1961–2002 for each track type. Yellow and red

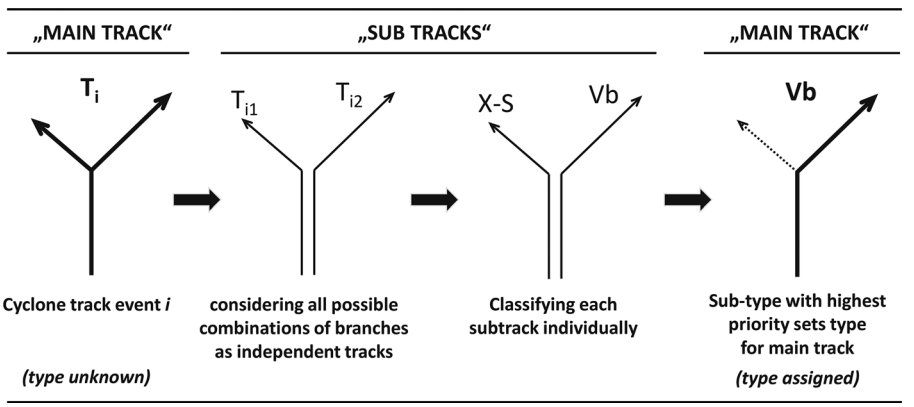

Figure 4. Procedure for identifying track type for split tracks (analogously for merge tracks).

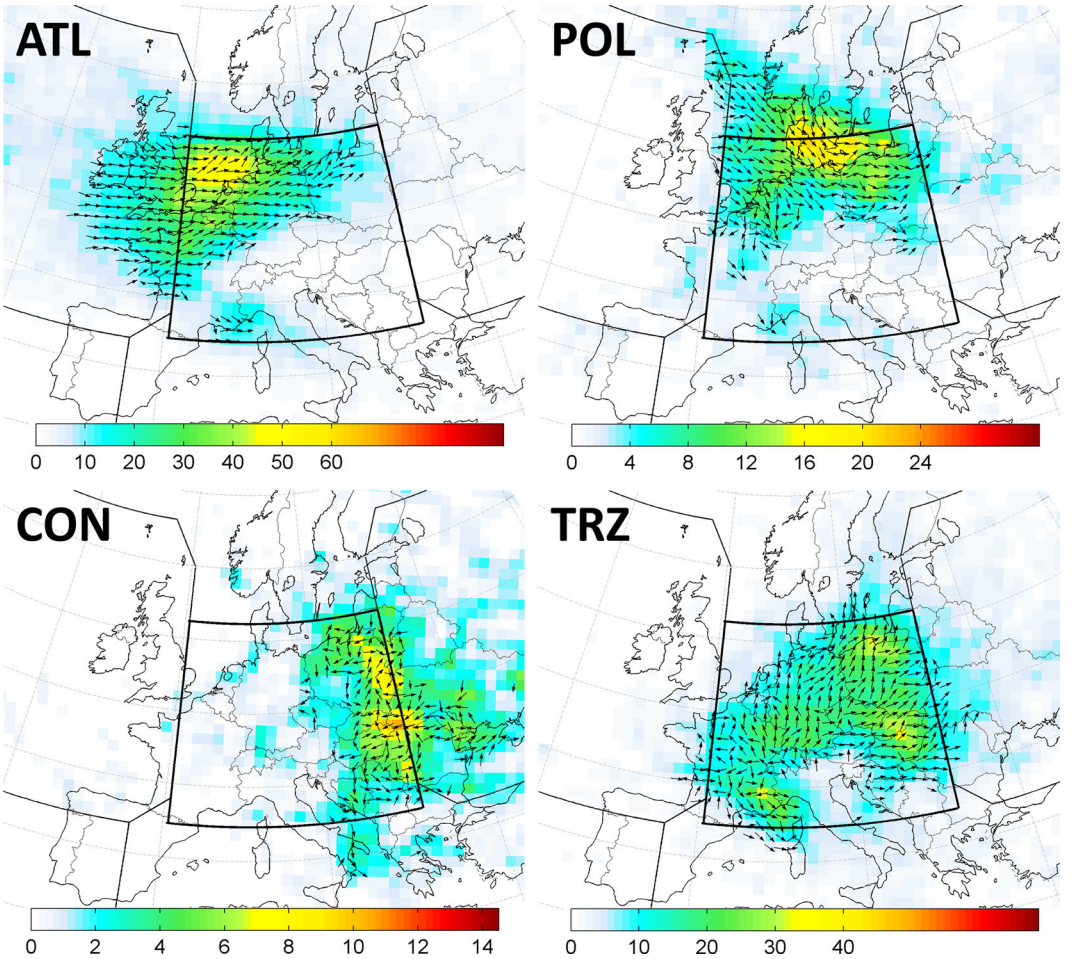

Figure 5. Track frequency (colors) for cyclone track types ATL, POL, CON, and TRZ at GPH700 (ERA-40, 1961–2002). Arrows indicate the mean direction of cyclone propagation. Numbers next to color bars indicate total number of cyclones recognized at a respective grid point for each track type in the analysis period.

cells refer to areas with a particularly large number of track passages, i.e., hot spots. Arrows, indicating the mean direction of cyclone propagation, have only been plotted for track frequencies above a threshold. ATL-type cyclones usually approach directly from the north-eastern Atlantic turning to the northeast over CE, with a pronounced frequency maximum over the southern parts of the North Sea. In contrast, Polar tracks (POL) have their maximum over Denmark with a clear propagation from northwest to southeast. For track type TRZ, there is no clear hot spot apparent, unlike most other types. A closer look at the synoptic situation during several major TRZ track events revealed that many of these cyclones originate over CE at SLP, induced by a major upper level trough located over western Europe. This also explains the strong northward component in the propagation of type TRZ cyclones.

The frequency map for Vb-type cyclones (Figure 6, top left) demonstrates that the current classification is very close to the original Vb path as defined by *van Bebber* [1891]. These cyclones emerge between the first frequency maximum near the Gulf of Lion and northern Italy and propagate to the northeast bypassing the eastern Alps, as intended by the classification (Figure 3b). Interestingly, there is a second maximum of cyclone frequency to the lee of the eastern Alps (western Hungary/Slovakia). This maximum might be related to a secondary cyclogenesis region in the eastward lee of the Alps, which has not been mentioned by other authors so far, presumably because this feature can only be seen when focusing on Vb-type tracks alone.

The frequency map for type X-S (Figure 6, bottom right) shows a very distinct region with numerous cyclone tracks over north-western Italy. These cyclones directly emerge on the leeside of the European Alps and propagate to the east into eastern Europe or to the southeast into the eastern Mediterranean Sea (see

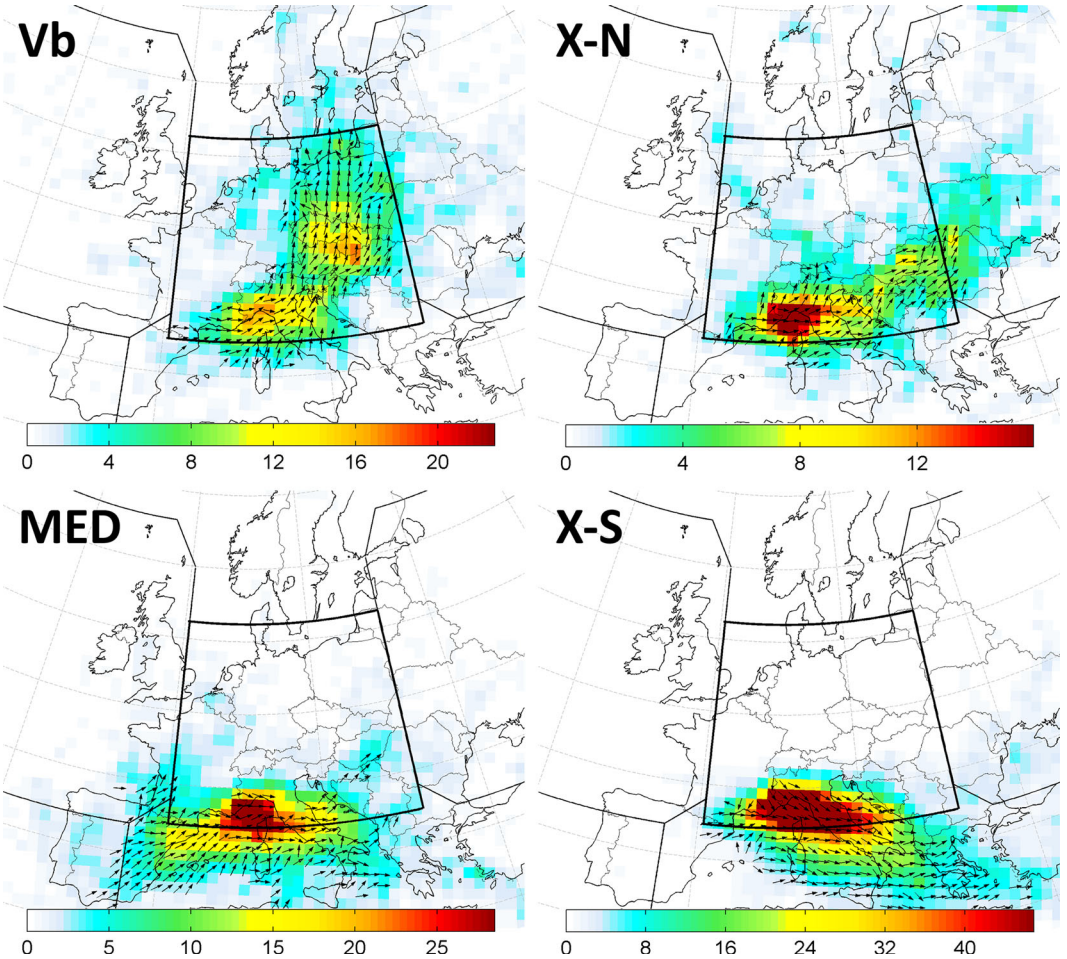

Figure 6. Same as Figure 5 but for cyclone track type Vb, X-N, X-S, and MED at GPH700 (1961–2002).

also Figure 7). The general propagation of X-S tracks is very different from that of type X-N. This is worth noting as these types are separated only by their mean propagation direction during the first 24 h, with no restrictions related to the subsequent movement. Overall, the typical propagation directions shown in Figure 6 correspond very well with a manual composite of propagation vectors for the western Mediterranean [*Campins et al.*, 2011] as well as with those presented by *Trigo et al.* [1999]. Track frequency maps for SLP (not shown) are similar to those at 700 hPa with the main difference that cyclones tend to move around major orographic features such as the Alps. Figure 7 shows the tracks of all cyclones by track type.

The mean annual number of cyclones per track type is presented in Table 3. On average, about 122 tracks per year are found at SLP and 83 tracks per year at GPH700 over CE. The smaller number of tracks at GPH700 is due to the smoother pressure patterns, despite the same spatial resolution and the prefiltering. Mountain ranges such as the Alps, Pyrenees, and Dinaric Alps, have a significant impact on the atmospheric flow, particularly at low levels [*Smith*, 1979], affecting the number and track locations of cyclones over Europe [*Egger and Hoinka*, 2008]. As regards the different track types, about 50% of all cyclones approach from the Atlantic to CE (type ATL, about 25%) or emerge directly over CE (type TRZ, about 25%). A substantial number of cyclones is of type X-S (about 20%), which are usually inside CE only during the first few time steps, i.e., in the initial phase. The remaining 30% of central European cyclones consist of the other types X-N, MED, Vb, CON, and POL. The number of SLP cyclone tracks originating within the region nas* or med* (type X-N, X-S, and Vb) south of the Alpine ridge is about 36 tracks per year, which corresponds very well with the number of cyclogenesis events found by *Campins et al.* [2011] around the Genoa region with about 37 events per year. Table 3

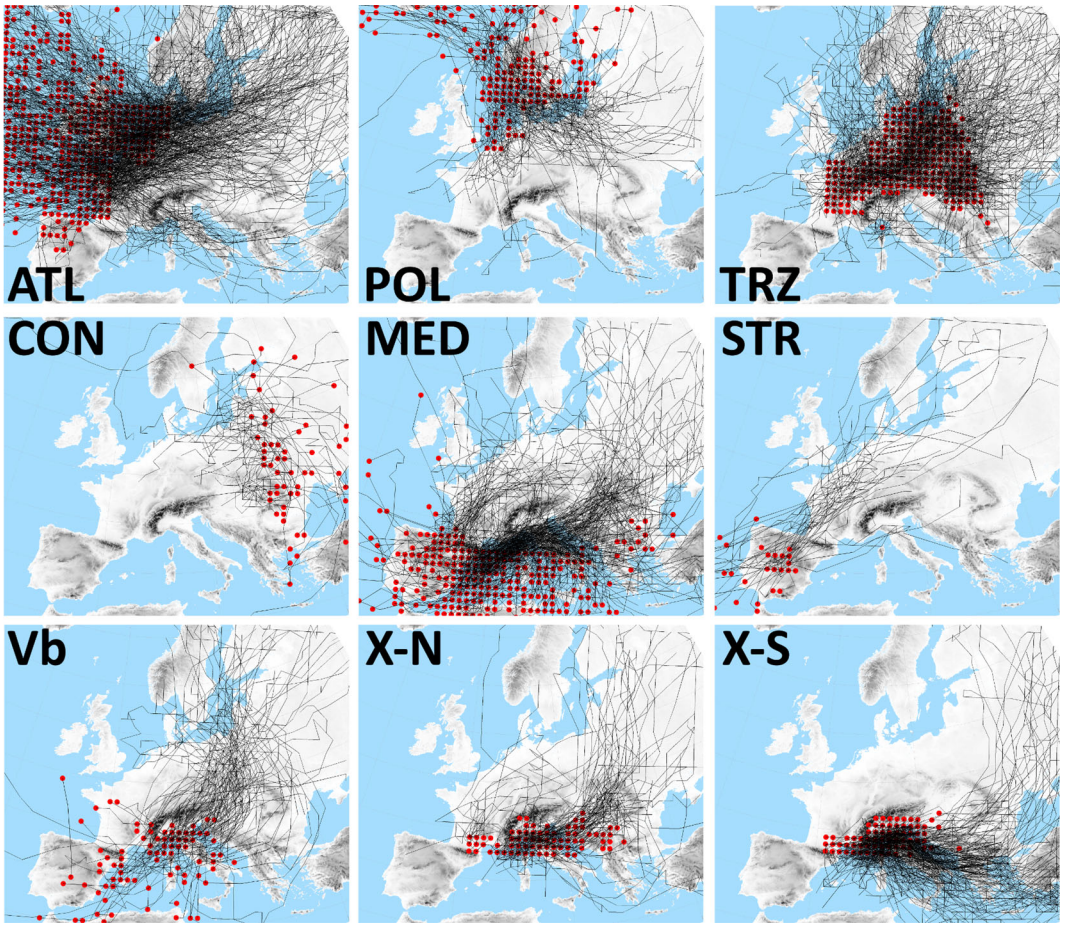

Figure 7. Members of the cyclone track types (SLP, 1961–2002). Red dots indicate the point of first detection of individual tracks.

also gives the frequencies of the strongest 10% of the cyclones (intensity $\xi > 90$th percentile). About 40%–55% of strong cyclones follow ATL-type tracks, which corresponds well with synoptic observations. For almost all of the other track types, the frequency is much lower (POL, MED, CON, X-N, and X-S), except for Vb where the relative frequency of strong cyclones is significantly higher than for all cyclones (7% as opposed to 3% at SLP, and 13% as opposed to 5% at GPH700).

Table 3. Cyclone Track Frequency[a]

	Mean Annual Number		Frequency			
			GPH700		SLP	
	GPH700	SLP	All (%)	Strong (%)	All (%)	Strong (%)
ATL	21.8	27.7	26	40	23	54
POL	7.2	6.5	9	10	5	7
CON	2.5	1.6	3	4	1	2
TRZ	20.2	32.6	24	14	27	7
Vb	4.1	3.1	5	13	3	7
X-N	4.6	7.7	6	4	6	2
X-S	14.8	25.2	18	10	21	9
MED	7.4	17.3	9	5	14	12
Total	82.6	121.7	100	100	100	100

[a]Frequencies (number of tracks for a type per total number of tracks) are given for all cyclones (all) and for strong cyclones (intensity $\xi > 90$th percentile) separately, rounded to percent integers. ERA-40 data (1961–2002).

3.2. Intensity Characteristics

Here selected climatological characteristics of cyclone intensity in terms of central air pressure and relative geostrophic vorticity are presented. The track types are investigated with respect to their life-cycle stage when entering CE. For all cyclones, six-hourly tendencies of vorticity and pressure are averaged over the first 24 h after a cyclone has entered TRZ. All cyclones with a significant (>75th percentile) change, in both tendencies, are grouped into either "intensifying" or "decaying." To be classified into the former group, both falling

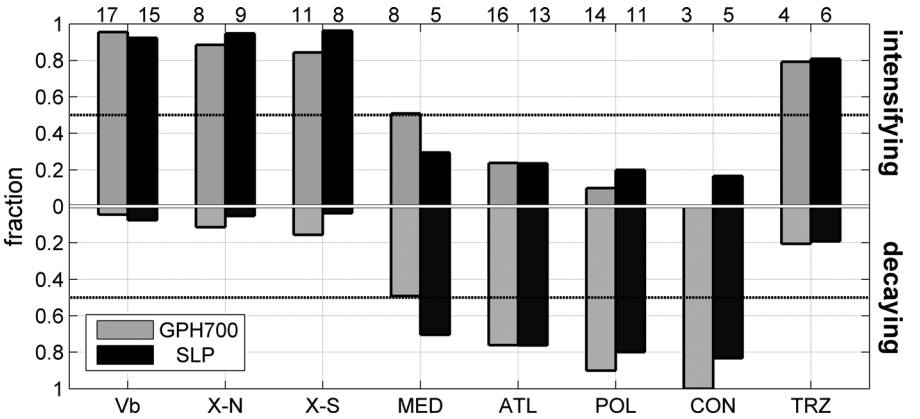

Figure 8. Fraction of cyclones that significantly intensify (upward bars) and decay (downward bars) during the first 24 h after entering central Europe (region TRZ) of all tracks with a strong change in both central pressure and relative vorticity. Numbers on top indicate the sample size as percentage for each track type.

pressure and increasing vorticity must occur, and vice versa for the latter group. About 10% of all cyclones at each level are classified as significantly changing. The results (Figure 8) show that cyclones of type Vb, X-N, X-S, or TRZ are usually intensifying when entering CE. Cyclones of type Vb, X-N, and X-S (i) strongly intensify over and (ii) originate from around the western Mediterranean Coast between the Rhône Valley and the Gulf of Genoa (not shown). As X-N and Vb cyclones move straight through or close by CE right after their intensification, they are expected to be closely related to high-impact weather events in CE. In contrast, most significantly changing cyclones of track types ATL, CON, and POL are already at a decay stage over CE, which is related to their genesis outside CE [e.g., *Wernli and Schwierz*, 2006]. The relative frequencies of the life cycle stages (intensification, decay) do not depend very much on the season, but appear to be an overall characteristic feature of the individual track type (not shown).

The fraction of intense cyclones is remarkably high for certain track types as shown before (Table 3), suggesting systematic differences in cyclone intensity between the types. Therefore, minimum central pressure and maximum relative vorticity of the cyclones during their location within TRZ are investigated in more depth for SLP (Figure 9). In winter (November–April, black bars), Atlantic and Vb-type cyclones are the most intense ones on average (low pressure and high vorticity), followed by CON and POL. However, ATL cyclones are usually stronger over the Atlantic Ocean than over central Europe (not shown). The most striking finding is the exceptionally high intensity of track type Vb during the summer half-year (May–October, gray bars). The 80th percentile of the relative geostrophic vorticity in summer is even above the corresponding value of ATL winter cyclones. Clearly, Vb-type cyclones are not only among the most intense and deepest central European cyclones, but particularly strong in the summer season. This may explain why Vb-type cyclones have been related to the most devastating floods in CE in recent decades, all of them occurring in the summer season, when equivalent-potential temperatures are usually high. However, the processes causing Vb cyclones to develop so strongly in the warm season are not fully clear, as the upper level steering flow over CE is significantly stronger in winter. Interestingly, *Trigo et al*. [2002] found that cyclones evolving from the region of Genoa, such as the Vb type, are more intense in winter mainly due to dynamic forcing between the Alps and the atmospheric flow, whereas low-level baroclinity plays a secondary role. They also observed a large number of significant summer cyclogenesis events in the region of Genoa, often when the upper level dynamic forcing acted at the time of the local thermal daily maximum in the late afternoon, especially in August [*Trigo et al*., 2002]. This corresponds with the findings of *Aebischer and Schär* [1998], with latent heating at low to intermediate levels, resulting from water vapor condensation, contributing significantly to frontogenesis and cyclogenesis on the lee-side of the Alps over northern Italy. High equivalent potential temperatures over northern Italy over the Po Plain may therefore be an essential prerequisite for the formation of exceptionally strong cyclones evolving in the summer season over northern Italy.

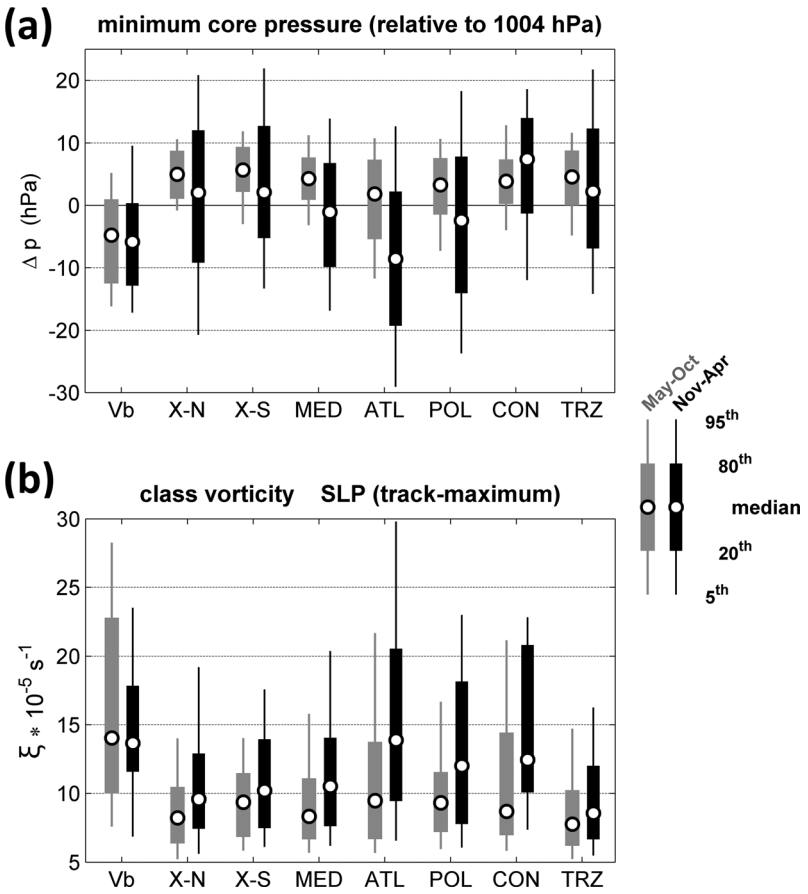

Figure 9. Climatological characteristics of cyclone track types at SLP in region TRZ (grey: May–October, black: November–April). (a) Minimum core pressure and (b) maximum relative vorticity.

4. Precipitation Related to Track Types

The classification scheme of cyclone tracks can be used for a range of analyses relevant to regional hydrology. Here for space reasons, only a brief analysis with respect to long-term precipitation totals as well as selected flood events is presented as a proof of concept. More detailed analyses will be presented in future publications.

4.1. Long-Term Precipitation Totals

In a first analysis, we examine the effect of the cyclones on precipitation totals in the focus region (Germany, Austria, parts of Switzerland and the Czech Republic). During the time, a cyclone was within TRZ, daily precipitation from the HYRAS and GPARD-6 data at a given grid point was assigned to that track type and accumulated over all cyclones of the same type, irrespective of the level. Precipitation of less than 1 mm per grid point and day has been disregarded. If a cyclone was located within TRZ only for a part of a day on a given date (6, 12, or 18 h), daily precipitation was weighted according to the fraction of time (0.25, 0.5, or 0.75). The results of this analysis are eight maps of precipitation totals during 1961–2002 associated with the nine track types.

As indicated earlier (Table 3), an average of 83 and 122 cyclones per year have crossed central Europe as identified from the levels of 700 hPa and SLP. These cyclones (all types, both levels) account for a total of 46%–76% of observed precipitation in the focus region (Figure 10), depending on the location, with an average of 62%. If the pressure levels are analyzed solely, the percentages are 54% and 37% for SLP and 700 hPa, respectively. This difference arises from the larger number of cyclones at SLP as well as from the enhanced lifting of low-level moist air associated with cyclones extending down to the surface.

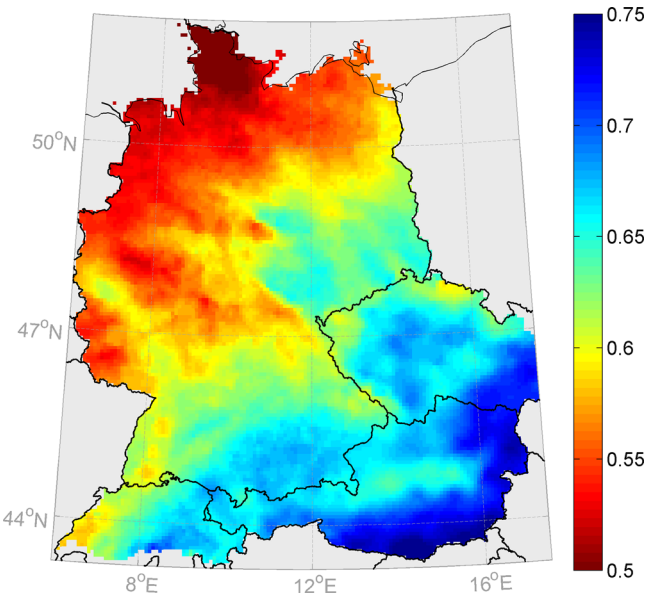

Figure 10. Fraction of precipitation attributed to the cyclones identified from 700 hPa and from SLP (1961–2002).

The identified cyclones capture a large part of the rainfall in the area (62%), although the percentage of days, where a cyclone is moving through TRZ and precipitation is observed, is only 20%–36%, depending on the location, with an average of 26% or 97 days per year. The overall number of days with precipitation is 131 days per year (ranging from 91 to 171), in contrast to 180 days per year on which a cyclone moves through CE, so nearly 50% (83 days) of all track days are dry days. For the remaining part of a year (151 days), there is no track and no precipitation has been observed. The fraction of total precipitation associated with cyclones over central Europe (62%) obtained here fits very well with other studies which attributed around 65% of the annual precipitation to stratiform type precipitation over the Czech Republic [*Rulfová and Kyselý*, 2013] and the Spanish Mediterranean Coast [*Ruiz-Leo et al*., 2013]. Over central Europe, the annual proportion of precipitation that occurs during cyclones ranges from 55% to 70% in summer and is about 75% in winter [*Hawcroft et al*., 2012] and between 60% and 70% were found to be associated with atmospheric fronts [*Catto et al*., 2012]. The fraction of precipitation accounted for here depends on the location and is largest in the southeast of the focus region and smallest in the north. This spatial pattern cannot be explained by different proximities to the border of the TRZ, as the focus region is centered on the middle of TRZ at 47°N and 12°E. Rather, cyclones in the northern part of TRZ are able to trigger precipitation in the south, while the opposite is not the case. Cyclones that have not been recognized inside TRZ are able to cause precipitation in the north-western part of the focus region, which is not counted in the analysis. This indicates that cyclones from the East Atlantic or North Sea have a larger spatial extent on average and are therefore able to reach into central Europe over large distances. Precipitation also occurs in the absence of atmospheric cyclones or in weak gradient situations with ill-defined cyclone centers which may contribute to the pattern of Figure 10. Typically, however, such situations favor convective type precipitation and should therefore affect both the south and the north of the focus region.

One of the motivations of the classification has been the expectation that cyclone track types differ in their precipitation characteristics. Figure 11 shows mean precipitation for each track type, relative to the mean precipitation without stratification by type. The average precipitation over the focus region for days with cyclones traversing TRZ was found as 2.88 mm/d, which is between the estimates of 2 mm/d [*Hawcroft et al*., 2012] and 4 mm/d [*Catto et al*., 2012] for central Europe. The number of 2.88 mm/d may appear small, but is an average over the whole focus region (545,000 km^2) and all cyclone track dates, so includes numerous instances/locations without precipitation. The majority of cyclones are not associated with significant precipitation and only a small number of cyclones accounts for most of the annual total precipitation.

Track types ATL, Vb, X-N, X-S, STR, and MED are associated with above average precipitation (3.66, 3.62, 3.50, 3.23, and 3.12 mm/d, respectively) as an average over the whole domain. In contrast, track types POL, TRZ, and CON are associated with below average precipitation of (2.60, 2.59, and 1.56 mm/d, respectively). For some of the track types, there are very clear spatial precipitation patterns that differ drastically between the track types, with even higher amounts in specific parts of the focus region. For example, ATL cyclones usually affect the western part of the focus region and cease in the eastern lee

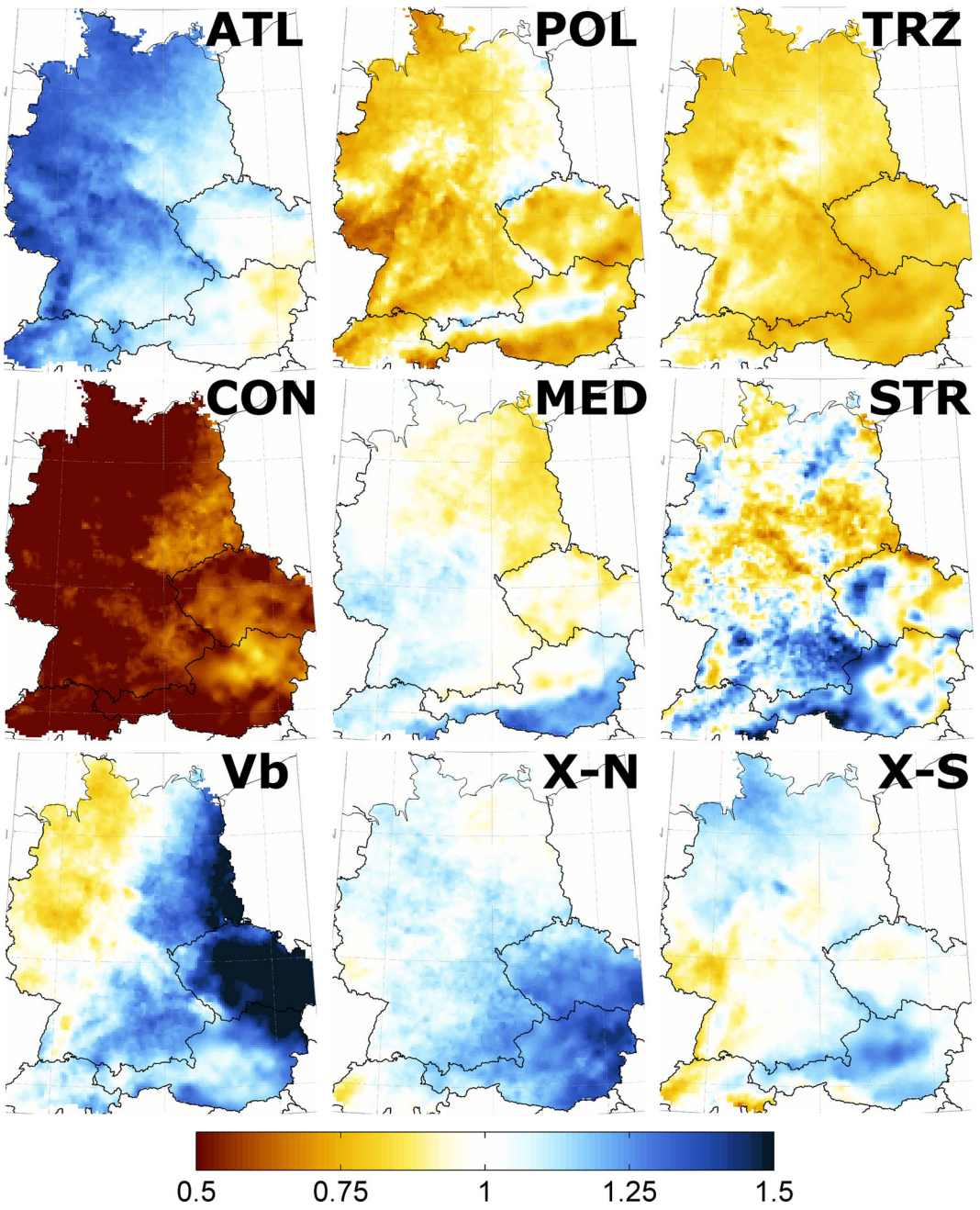

Figure 11. Ratio of mean precipitation of each track type and mean precipitation of all tracks. This ratio indicates track types and regions with high (blue) or low (brown) contributions to precipitation associated with cyclones over central Europe.

of the central European mountain ranges. This pattern matches very well with climatology, where annual precipitation totals decrease from western to eastern Europe, in line with a weakened influence of Atlantic weather regimes.

POL cyclones have the strongest positive anomalies (a maximum of 3.89 mm/d) in the northern stau regions of the Erzgebirge and Alps (light blue bands in Figure 11), implying a strong northerly flow against the orography and related lifting of moist air. MED cyclones show a stronger signal (max = 4.51 mm/d) in the regions south of the Alpine range (in the very south of the focus region). STR shows a noisy pattern, which can be related to the dominance of convective type precipitation leading to local minima and maxima over the domain (max = 5.34 mm/d). High-precipitation totals are found for ATL cyclones in the western

Table 4. Significant Precipitation Events and Track Types[a]

Region→	NW-Germany		S-Germany, N-Austria		Czech Republic, W-Slovakia, SW-Poland	
Catchments→	Neckar, Main, Moselle, Ems, Aller, Weser		Upper-Danube, Inn, Enns		Vltava, Elbe, Oder, Morava, Váh	
Precipitation Event	SLP	GPH700	SLP	GPH700	SLP	GPH700
11 Jun 1965	TRZ	TRZ	TRZ	TRZ	TRZ	TRZ
18 Jul 1965	TRZ	TRZ				
5 Dec 1970	TRZ	TRZ				
19 Jul 1970					TRZ	Vb
11 Aug 1970			X-S	X-S		
22 Aug 1972					TRZ	Vb
24 Jun 1973			X-N	ATL		
2 Jul 1975			X-N	POL		
1 Aug 1977			Vb	Vb	Vb	Vb
24 May 1978	MED	X-N				
10 Oct 1980					Vb	Vb
6 Jul 1981	TRZ	TRZ				
2 Jul 1981	Vb	ATL				
21 Jul 1981			Vb	Vb	Vb	Vb
13 Aug 1981	TRZ	TRZ				
26 May 1983	TRZ	*				
7 Aug 1983					X-N	ATL
2 Jul 1984	TRZ	ATL				
7 Aug 1985			Vb	Vb	Vb	Vb
24 Oct 1986	ATL	ATL				
6 Oct 1993	TRZ	TRZ				
8 Jul 1997			TRZ	X-N	TRZ	X-N
29 Oct 1998	ATL	*				
13 May 1999			TRZ	TRZ		
22 May 1999			Vb	X-S		
12 Aug 2002			Vb	Vb	Vb	Vb

[a]Most significant precipitation events over selected parts of central Europe for the summer half years (May–October) between 1961 and 2002 (adapted from *Müller et al*. [2009]) and attribution to cyclone track types. Empty fields indicate that the event is not among the top events in the respective catchment. Asterisk indicates that the event is not recognized as a cyclone moving into TRZ.

parts of Germany and Switzerland (max = 4.30 mm/d), for X-N cyclones (max = 4.86 mm/d) in the south-eastern parts of CE (Austria and Czech Republic). The clearest pattern appears for Vb cyclones with very high precipitation contributions over a large area in the Czech Republic (max = 5.82 mm/d). Vb cyclones develop around Genoa and move around the eastern Alps toward Poland. Moisture is advected toward the mountains in an anticlockwise rotation and frontal lifting is intensified through orographic enhancement. As a result, very large precipitation depths are observed in the regions located along or west of the Vb cyclone track. Another reason for the large precipitation depths is the strong intensity of Vb cyclones (Figure 9).

4.2. Heavy Precipitation Events From 1961 to 2002

Major flood events in central Europe are often attributed to particular cyclone types such as Vb. To demonstrate the practical applicability of the new cyclone track classification, the nine track types are attributed here to the most significant precipitation events in selected river basins in central Europe. *Müller et al*. [2009] published a list of significant precipitation events for 25 river basins. The events were selected on the basis of runoff peaks compared to average flow conditions within the summer half years in the period 1951–2002. These events are listed in Table 4 for the period 1961–2002, along with the associated cyclone track type identified in the present study. The table shows that, in northwestern Germany (Neckar, Main, Moselle, Ems, Aller, and Weser rivers), 11 out of 12 events are associated with ATL or TRZ tracks and the remaining events are associated with tracks starting in the western Mediterranean (MED, Vb, or X-N). In southern Germany and northern Austria (Upper-Danube, Inn, and Enns rivers), some, but fewer, events can be attributed to TRZ, ATL, or POL but a significant number to X-S, X-N, or Vb. The latter are cyclones that mainly develop on the southern lee-side of the Alps.

In the Czech Republic, western Slovakia and southwestern Poland (Vltava, Elbe, Oder, Morava, and Váh rivers) almost all of the significant precipitation events are connected to Vb cyclone tracks. Overall, this fits very well with the findings above, where the extreme intensity characteristics already pointed to Vb as a very special track type over central Europe. For most of the events associated with TRZ tracks, either a cyclone was found developing at the northern or southern lee-side of the Alps at SLP, or a stationary cutoff low was found at higher atmospheric levels over CE. This comparison also indicates that the connection between track types and heavy precipitation is not uniform in space and may also depend on the season. With two exceptions at 700 hPa (indicated by an asterisk in Table 4) all precipitation events can be associated with cyclones identified in this study, which adds credence to the consistency of the approach. For most of these events, the same cyclone track type was found at SLP and 700 hPa atmospheric levels, but there are a number of events where the track types are not consistent

between the levels. Different cyclone paths can typically be observed when the vertical axis of a cyclone is tilted, for example, when the upper level trough amplifies and decelerates while the surface cyclone still moves ahead or circles around the upper level trough. In other cases, a major upper level trough approaches from the Atlantic and steers the formation of a new surface level cyclone with a different track type over central Europe. Examples are the events on 2 July 1981, 7 August 1983, and 2 June 1984 in Table 4.

5. Discussion of Classification Results

5.1. Southern Alpine Track Types in Comparison

A first assessment of the classification approach is performed by comparing the similar track types Vb, X-N, and X-S. These types predominantly emerge from the western Mediterranean Sea—south of the Alpine ridge—with a general propagation to easterly directions in the course of their life time (Figure 7). The average number of cyclones per year is very different between these three types, with a total number of 3.1 (Vb), 7.7 (X-N), and 25.2 (X-S) cyclones per year for SLP. The number of Vb cyclones per year for the two levels are 3.1 and 4.1 at SLP and GPH700, respectively, which is similar to results from the literature based on ERA-40 data with 3.0 at GPH700 [*Kummli*, 2014], and 3.5 at GPH700 [*Hofstätter and Chimani*, 2012]. A significantly lower count of Vb-type cyclones at SLP was found by *Nissen et al*. [2014] but they used a different recognition approach. As can be seen from Figure 7, type X-S shows a reasonable similarity to X-N, as a significant part of the former turn back to the north at some point, despite the restriction in the classification of a southward direction after recognition. This means that X-N and X-S do not necessarily have to be considered as different types in the early development phase as intensity (Figure 9), and intensity change (Figure 8) characteristics are not very different either. However, distinguishing these two types may be important if one is interested in a region further to the southeast, e.g., the Balkan region. Type X-N looks very similar to Vb, especially in terms of the propagation paths southeast of the Alpine ridge and the points of first detection, however, Vb tracks turn to the north approaching central Europe more closely. This may be related to characteristic upper level cutoff lows located over CE [*Grams et al*., 2014] in case of Vb which, presumably, is not a dominant feature for X-N. A separation of the three track types therefore appears meaningful.

5.2. Sensitivity Experiment for Classifying Vb

As the number of Vb-type cyclones is low as compared to type X-N and X-S, and Vb tracks have similar, eastbound propagation paths as X-N (see Figure 7), a sensitivity experiment is carried out by varying the width of region "$x_{(tn)}$" through the boundaries in the east and west (see Figure 3 for the original setup), and reapplying the classification procedure to SLP. The experiment shows that the number of Vb-type cyclones is somewhat sensitive to the eastward extent but almost not to the westward extent (Table 5). When changing the eastward boundary from 20°E (original setup) to 23°E, the number of Vb cyclones increases by about 20% per degree increment. Virtually all additional cyclones classified as Vb in this case are at the expense of X-N and X-S in equal shares. At the level of 700 hPa, the effect of altered boundaries is even smaller than at SLP (not shown). The sensitivity of the track number to the definition of the region suggests that preferred track streams do exist over CE but the spatial transition between different types is a smooth one.

6. Conclusions

In this paper, a procedure for tracking atmospheric cyclones has been adapted to ERA-40 data over Europe for the purpose of this study. A new classification approach is proposed for separating tracks into nine

Table 5. Sensitivity of Classification to Vb Tracks[a]

	Extended Westward Boundary		Original Setup[b]	Extended Eastward Boundary				
	12°	13°/–	14°/20°	–/20.25°	–/20.5°	–/21°	–/22°	–/23°
Events per year	3.3	3.2	3.1	3.5	3.7	4.0	4.5	4.9

[a]Mean annual number of Vb-type cyclone tracks for different longitudinal sizes of region "$x_{(tn)}$." ERA-40 data, 1961–2002, SLP.
[b]Original size 14°E–20°E as shown in Figure 3b.

types, based on the geographical regions from where the cyclones propagate into central Europe (CE). The regions were defined by large geographical domains with a consistent topography and similar surface characteristics, based on a priori knowledge from synoptic observations.

The resulting cyclone track types show distinct properties in terms of frequency and intensity. Atlantic cyclones and cyclones developing directly over CE (type TRZ) are the most frequent ones (about 25% relative frequency each), which is in good agreement with synoptic observations. Cyclones developing in the northern parts of the Mediterranean on the lee-side of the Alps (types Vb, X-N, and X-S) have a combined frequency of 25%. The remaining cyclones are classified as CON, POL, and MED types. Strong cyclones, both in terms of relative geostrophic vorticity and central pressure, are found among ATL, Vb, POL, and CON tracks in the winter half year. More importantly, the frequency of strong Vb cyclones is particularly high during the summer half year, which can be explained by additional cyclogenetic processes acting on the lee-side of the Alps, as latent heat release at lower levels [*Aebischer and Schär*, 1998] or frontogenetic low-level wind convergence [*Horvath et al*., 2008], but not by dominant dynamic forcing between upper level winds and the Alps alone, as is usually the case in winter. The study also strongly suggests the existence of preferred cyclone propagation paths over CE. Although these are usually affected by the underlying topography, specific dominant upper level circulation patterns may also play an important role for the within-type characteristics.

The new cyclone track catalog has the potential for interesting follow-up investigations on climatological characteristics, the temporal behavior and the relevance of track types for extreme precipitation in CE. As a proof of concept, long-term precipitation totals are analyzed stratified by track types here. Track types ATL, Vb, X-N, and X-S are associated with above average precipitation while track types CON, STR, POL, and TRZ are associated with below average precipitation. The contributions of the track types to precipitation totals differ enormously in space. This suggests that the risk of heavy precipitation over central Europe very much depends on the specific cyclone track type and location. A comparison of significant precipitation events [from *Müller et al*., 2009] with cyclone track types shows that almost all of the events have been identified by the proposed scheme. In south-western Poland, Czech Republic and western Slovakia 7 of the top 10 precipitation events can be attributed to Vb tracks.

Of course there are limitations to the approach and caveats in the applicability of the new track types which opens up room for new research. First, the approach has been applied independently to data from two atmospheric levels, SLP and GPH700. Although tracking studies are usually based on one single level, the creation of a consistent and unique track catalog, combining information from different levels has potential and should be pursued in the future. The initial size of the tracking domain does not capture the eastern Atlantic region to its full extent. While Atlantic-type cyclones are correctly classified, some tracks may not be detected from the very beginning. This is not considered relevant to this study but could be to others. In this study, precipitation is always attributed to a cyclone moving through region TRZ, irrespective of the distance to the cyclone, its spatial extent and the location of the atmospheric front associated with the cyclone. By incorporating this kind of information even more detailed spatial patterns could be identified. Finally, it should be mentioned that the number of tracks identified is not fully independent between the different types, as certain geographical regions are given higher priority than others in the classification. If a track includes branches, the subtrack from high priority regions determines the type of the entire track-complex and the other subtracks (branches) are disregarded. This applies to 10% of all tracks, with a higher proportion at SLP during the summer season and/or during weak gradient situations.

The cyclone track classification presented in this study is optimized for the central European domain. However, the basic concept behind the classification can readily be transferred to other midlatitude and possibly tropical regions of the world by adapting the setup according to local synoptic information, and their effect on precipitation [e.g., *Steinschneider and Lall*, 2015; *Huang Jr et al*., 2012]. Further research could also focus on the characteristics of continental-scale processes controlling the formation, propagation and transformation of central European cyclones by examining distinct track types. In subsequent studies, a climatology of European cyclone tracks, as classified with the current approach, will be presented and the track types will be related to extreme precipitation in central Europe.

Acknowledgments
ECMWF ERA-40 data used in this study have been obtained from the ECMWF data server (http://apps.ecmwf.int/datasets/). The precipitation data are available from DWD and ZAMG on request. Data on cyclone tracks are available on personal request from ZAMG/Michael Hofstätter (e-mail: m.hofstaetter@zamg.ac.at). This study has been funded by the Austrian Ministry of Life—Department for Water Affairs and the Bavarian State Ministry of the Environment and Public Health. We also acknowledge financial support from the Austrian Science Funds (FWF) as part of the Vienna Doctoral Programme on Water Resource Systems (DK-plus W1219-N22) and the ERC Advanced Grant "Flood Change," Project 291152. The authors would like to thank the three anonymous reviewers for their constructive comments and helpful suggestions on an earlier version of the manuscript.

References

Aebischer, U., and C. Schär (1998), Low-level potential vorticity and cyclogenesis to the lee of the Alps, *J. Atmos. Sci.*, *55*, 186–207, doi:10.1175/1520-0469(1998)055<0186:LLPVAC>2.0.CO;2.

Akima, H. (1978), A method of bivariate interpolation and smooth surface fitting for irregularly distributed data points, *ACM Trans. Math. Software*, *4*, 148–164, doi:10.1145/355780.355786.

Akima, H. (1996), Algorithm 761: Scattered-data surface fitting that has the accuracy of a cubic polynomial, *ACM Trans. Math. Software*, *22*, 362–371, doi:10.1145/232826.232856.

Apostol, L. (2008), The Mediterranean cyclones—The role in ensuring water resources and their potential of climatic risk in the east of Romania, *Present Environ. Sustainable Dev.*, *2*, 143–163.

Bengtsson, L., K. I. Hodges, and E. Roeckner (2006), Storm tracks and climate change, *J. Clim.*, *19*, 3518–3543, doi:10.1175/JCLI3815.1.

Blender, R., K. Fraedrich, and F. Lunkeit (1997), Identification of cyclone track regimes in the North Atlantic, *Q. J. R. Meteorol. Soc.*, *123*(539), 727–741, doi:10.1002/qj.49712353910.

Blöschl, G., T. Nester, J. Komma, J. Parajka, and R. A. P. Perdigão (2013), The June 2013 flood in the Upper Danube basin, and comparisons with the 2002, 1954 and 1899 floods, *Hydrol. Earth Syst. Sci. Discuss.*, *10*, 9533–9573, doi:10.5194/hess-17-5197-2013.

Buzzi, A., and S. Tibaldi (1978), Cyclogenesis in the lee of the Alps: A case study, *Q. J. R. Meteorol. Soc.*, *104*, 271–287, doi:10.1002/qj.49710444004.

Campins, J., A. Jansà, and A. Genovés (2006), Three-dimensional structure of western Mediterranean cyclones, *Int. J. Climatol.*, *26*(3), 323–343, doi:10.1002/joc.1275.

Campins, J., A. Genovés, M. A. Picornell, and A. Jansà (2011), Climatology of Mediterranean cyclones using the ERA-40 dataset, *Int. J. Climatol.*, *31*, 1596–1614, doi:10.1002/joc.2183.

Catto, J. L., C. Jakob, G. Berry, and N. Nicholls (2012), Relating global precipitation to atmospheric fronts, *Geophys. Res. Lett.*, *39*, doi:10.1029/2012GL051736.

Dacre, H. F., and S. L. Gray (2009), The spatial distribution and evolution characteristics of North Atlantic cyclones, *Mon. Weather Rev.*, *137*, 99–115, doi:10.1175/2008MWR2491.1.

Davis, R. E., G. Demme, and R. Dolan (1993), Synoptic climatology of Atlantic coast North-Easters, *Int. J. Climatol.*, *13*(2), 171–189, doi:10.1002/joc.3370130204.

Dee, D. P., et al. (2011), The ERA-Interim reanalysis: Configuration and performance of the data assimilation system, *Q. J. R. Meteorol. Soc.*, *137*, 553–597, doi:10.1002/qj.828.

Donat, M. G., G. C. Leckebusch, J. G. Pinto, and U. Ulbrich (2010), Examination of wind storms over Central Europe with respect to circulation weather types and NAO phases, *Int. J. Climatol.*, *30*, 1289–1300, doi:10.1002/joc.1982.

Egger, J., and K. P. Hoinka (2008), Mountain torques and synoptic systems in the Mediterranean, *Q. J. R. Meteorl. Soc.*, *134*, 1067–1081, doi:10.1002/qj.248.

Freser, F., and H. von Storch (2005), A spatial two-dimensional discrete filter for limited-area-model evaluation purposes, *Mon. Weather Rev.*, *133*, 1774–1786, doi:10.1175/MWR2939.1.

Grams, C. M., H. Binder, S. Pfahl, N. Piaget, and H. Wernli (2014), Atmospheric processes triggering the central European floods in June 2013, *Nat. Hazards Earth Syst. Sci.*, *14*, 1691–1702, doi:10.5194/nhess-14-1691-2014.

Hanley, J., and R. Caballero (2012), Objective identification and tracking of multicentre cyclones in the ERA-Interim reanalysis dataset, *Q. J. R. Meteorl. Soc.*, *138*, 612–625, doi:10.1002/qj.948.

Hawcroft, M. K., L. C. Shaffrey, K. I. Hodges, and H. F. Dacre (2012), How much Northern Hemisphere precipitation is associated with extratropical cyclones?, *Geophys. Res. Lett.*, *39*, L24809, doi:10.1029/2012GL053866.

Hewson, T. D., and H. A. Titley (2010), Objective identification, typing and tracking of the complete life-cycles of cyclonic features at high spatial resolution, *Meteorl. Appl.*, *17*, 355–381, doi:10.1002/mct.204.

Hofstätter, M., and B. Chimani (2012), van Bebber's cyclone tracks at 700 hPa in the eastern Alps for 1961–2002 and their comparison to Circulation Type Classifications. *Meteorl. Z.*, *21*(5), 459–473, doi:10.1127/0941-2948/2012/0473.

Hofstätter, M., J. Jacobeit, M. Homann, A. Lexer, B. Chimani, A. Philipp, C. Beck, and M. Ganekind (2015), WETRAX – Weather Patterns, Cyclone Tracks and related Precipitation Extremes, Großflächige StarkniederschlûÊge im Klimawandel in Mitteleuropa, Final Report, *Geographica Augustana, no. 19*, Universität Augsburg, Augsburg.

Huang, C., Jr., C. K. Yu, J. Y. Lee, L. W. Cheng, T. Y. Lee, and S. J. Kao (2012), Linking typhoon tracks and spatial rainfall patterns for improving flood lead time predictions over a mesoscale mountainous watershed, *Water Resour. Res.*, *48*, W09540, doi:10.1029/2011WR011508.

Horvath, K., Y. L. Lin, and B. Ivančan-Picek (2008), Classification of cyclone tracks over the Apennines and the Adriatic Sea, *Mon. Weather Rev.*, *136*, 2210–2227, doi:10.1175/2007MWR2231.1.

Hoskins, B. J., and K. I. Hodges (2002), New perspectives on the Northern Hemisphere winter storm tracks, *J. Atmos. Sci.*, *59*(6), 1041–1061, doi:10.1175/1520-0469(2002)059<1041:NPOTNH>2.0.CO;2.

Kalnay, E., et al. (1996), The NCEP/NCAR 40-year reanalysis project, *Bull. Am. Meteorol. Soc.*, *77*, 437–471, doi:10.1175/1520-0477(1996)077<0437:TNYRP>2.0.CO;2.

Klein, W. (1957), Principal tracks and mean frequencies of cyclone and anticyclones in the Northern Hemisphere, *Res. Pap. 40*, U.S. Weather Bur., Washington, D. C.

Kummli, C. (2014), Sensitivity of precipitation to Mediterranean SSTs in the case of the Vb-type cyclone in August 2005 using the regional model WRF, MS thesis, 95 pp., Fac. of Sci., Univ. of Bern, Bern, Switzerland.

Lim, E. P., and I. Simmonds (2007), Southern Hemisphere winter extratropical cyclone characteristics and vertical organization observed with the ERA-40 reanalysis data in 1979-2001, *J. Clim.*, *20*, 2675–2690, doi:10.1175/JCLI4135.1.

Müller, M., M. Kašpar, and J. Matschullat (2009), Heavy rains and extreme rainfall-runoff events in Central Europe from 1951 to 2002, *Nat. Hazards Earth Syst. Sci.*, *9*, 441–450, doi:10.5194/nhess-9-441-2009.

Murray, R., and I. Simmonds (1991), A numerical scheme for tracking cyclone centres from digital data. Part I: Development and operation of the scheme, *Aust. Meteorl. Mag.*, *39*, 155–166.

Nissen, K. M., U. Ulbrich, and G. Leckebusch (2014), Vb cyclones and associated rainfall extremes over Central Europe under present day and climate change conditions, *Meteorl. Z.*, *22*(6), 649–660, doi:10.1127/0941-2948/2013/0514.

Pichler, H., and R. Steinacker (1987), On the synoptics and dynamics of orographically induced cyclones in the Mediterranean, *Meteorol. Atmos. Phys.*, *36*(1-4), 108–117, doi:10.1007/BF01045144.

Pinto, J. G., T. Spangehl, U. Ulbrich, and P. Speth (2005), Sensitivities of a cyclone detection and tracking algorithm: Individual tracks and climatology, *Meteorl. Z.*, *14*, 823–838, doi:10.1127/0941-2948/2005/0068.

Rauthe, M., H. Steiner, U. Riediger, A. Mazurkiewicz, and A. Gratzki (2013), A Central European precipitation climatology—Part I: Generation and validation of a high-resolution gridded daily data set (HYRAS), *Meteorl. Z.*, *22*, 235–256, doi:10.1127/0941-2948/2013/0436.

Renard, B., and U. Lall (2014), Regional frequency analysis conditioned on large-scale atmospheric or oceanic fields, *Water Resour. Res.*, *50*, 9536–9554, doi:10.1002/2014WR016277.

Roberts, J. F., et al. (2014), The XWS open access catalog of extreme European windstorms from 1979 to 2012, *Nat. Hazards Earth Syst. Sci.*, *14*, 2487–2501, doi:10.5194/nhess-14-2487-2014.

Ruiz-Leo, A. M., E. Hernandez, S. Queralt, and G. Maqueda (2013), Convective and stratiform precipitation trends in the Spanish Mediterranean coast, *Atmos. Res.*, *119*, 46–55, doi:10.1016/j.atmosres.2011.07.019, 2013.

Rulfová, Z., and J. Kyselý (2013), Disaggregating convective and stratiform precipitation from station weather data, *Atmos. Res.*, *134*, 100–115, doi:10.1016/j.atmosres.2013.07.015.

Schröter, K., M. Kunz, F. Elmer, B. Mühr, and B. Merz (2014), What made the June 2013 flood in Germany an exceptional event? A hydro-meteorological evaluation, *Hydrol. Earth Syst. Sci. Discuss.*, *11*, 8125–8166, doi:10.5194/hess-19-309-2015.

Sinclair, M. R. (1994), An objective cyclone climatology for the southern Hemisphere, *Mon. Weather Rev.*, *122*, 2239–2256, doi:10.1175/1520-0493(1994)122<2239:AOCCFT>2.0.CO;2.

Sinclair, M. R. (1997), Objective identification of cyclones and their circulation intensity, and climatology, *Weather Forecasting*, *12*, 595–612, doi:10.1175/1520-0434(1997)012<0595:OIOCAT>2.0.CO;2.

Simmonds, I., R. J. Murray, and R. M. Leighton (1999), A refinement cyclone tracking methods with data from FROST, *Aust. Meteorol. Mag.*, Special edition, 35–49.

Smith, R. B. (1979), The influence of mountains on the atmosphere, *Adv. Geophys.*, *21*, 87–230, doi:10.1016/S0065-2687(08)60262-9.

Steinschneider, S., and U. Lall (2015), A hierarchical Bayesian regional model for nonstationary precipitation extremes in Northern California conditioned on tropical moisture exports, *Water Resour. Res.*, *51*, 1472–1492, doi:10.1002/2014WR016664.

Trigo, I. F., T. D. Davies, and G. R. Bigg (1999), Objective climatology of cyclones in the Mediterranean region, *J. Clim.*, *12*, 1685–1696, doi:10.1175/1520-0442(1999)012<1685:OCOCIT>2.0.CO;2.

Trigo, I. F., G. R. Bigg, and T. D. Davies (2002), Climatology of cyclogenesis mechanisms in the Mediterranean, *Mon. Weather Rev.*, *130*, 549–569, doi:10.1175/1520-0493(2002)130<0549:COCMIT>2.0.CO;2.

Ulbrich, U., T. Brücher, A. H., Fink, G. C. Leckebusch, A. Krüger, and J. G. Pinto (2003), The Central European Floods in August 2002, Part II: Synoptic causes and considerations with respect to climatic change, *Weather*, *58*, 434–441, doi:10.1256/wea.61.03B.

Uppala, S. M., et al. (2005), The ERA-40 re-analysis, *Q. J. R. Meteorol. Soc.*, *131*, 2961–3012, doi:10.1256/qj.04.176.

van Bebber, W. J. (1891), Die Zugstrassen der barometrischen Minima nach den Bahnenkarten der Deutschen Seewarte für den Zeitraum 1875–1890, *Meteorl. Z.*, *8*, 361–366.

Wernli, H., and C. Schwierz (2006), Surface cyclones in the ERA-40 dataset (1958–2001): Part I: Novel identification method and global climatology, *J. Atmos. Sci.*, *63*(10), 2486–2507, doi:10.1175/JAS3766.1.

Zahn, M., and H. von Storch (2008), Tracking polar lows in CLM, *Meteorol. Z.*, *17*(4), 445–453, doi:10.1127/0941-2948/2008/0317.